

# Space Object Detection using Multi-frame Temporal Trajectory Completion Method

Xiaoqing Lan

*School of Software*

*Northwestern Polytechnical University*  
Xi'an, China

lanxiaoqing@mail.nwpu.edu.cn

Biqiao Xin

*School of Software*

*Northwestern Polytechnical University*  
Xi'an, China

biqiaoxin@mail.nwpu.edu.cn

Bingshu Wang

*School of Software*

*Northwestern Polytechnical University*  
Xi'an, China

wangbingshu@nwpu.edu.cn

Han Zhang

*School of Artificial Intelligence,  
Optics and Electronics*

*Northwestern Polytechnical University*  
Xi'an, China

zhanghan9937@gmail.com

Rui Zhu

*National Key Laboratory of  
Space Target Awareness*

*Space Engineering University*  
Beijing, China

200347@hgd.edu.cn

Laixian Zhang\*

*National Key Laboratory of  
Space Target Awareness*

*Space Engineering University*  
Beijing, China

zhanglaixian@pku.edu.cn

**Abstract**—Space objects in Geostationary Earth Orbit (GEO) present significant detection challenges in optical imaging due to weak signals, complex stellar backgrounds, and environmental interference. In this paper, we enhance high-frequency features of GEO targets while suppressing background noise at the single-frame level through wavelet transform. Building on this, we propose a multi-frame temporal trajectory completion scheme centered on the Hungarian algorithm for globally optimal cross-frame matching. To effectively mitigate missing and false detections, a series of key steps including temporal matching and interpolation completion, temporal-consistency-based noise filtering, and progressive trajectory refinement are designed in the post-processing pipeline. Experimental results on the public SpotGEO dataset demonstrate the effectiveness of the proposed method, achieving an  $F_1$  score of 90.14%.

**Index Terms**—Space objects, geostationary earth orbit, multi-frame temporal trajectory completion

## I. INTRODUCTION

The Geostationary Earth Orbit (GEO) constitutes a unique and crucial spatial orbital resource [1]–[4]. However, space objects in this orbit, such as defunct satellites and discarded rocket debris, pose potential threats to space security [5], [6]. Their specific imaging characteristics manifest as space objects with limited pixel occupancy, lacking discernible features in size, texture, and contour [7].

In 2020, the European Space Agency (ESA) and the University of Adelaide jointly launched a public challenge named SpotGEO, inviting global experts to develop computer vision algorithms for detecting space objects in low-cost telescope images [8]. The GEO object detection task is challenging due to factors such as faint target signals, stellar occlusion, and environmental interference [9].

This work is supported by the National Key Laboratory of Space Target Awareness (STA2024KGJ0202, STA2024KG0201), the National Natural Science Foundation of China (62576281,62406249), and the Natural Science Basic Research Program of Shaanxi (2024JCYBQN-0612). Corresponding author: Laixian Zhang (Email: zhanglaixian@pku.edu.cn)

Traditional approaches rely on image processing like transformation and energy accumulation to suppress stellar interference [10], while recent works adopt deep learning [11]–[13]. Representative methods include GEO-FPN with EfficientNet backbone [14], YOLO-based object detection [15], and hybrid designs combining single-frame detection with multi-frame post-processing [16]. Temporal attention mechanisms [17] and ConvLSTM frameworks [18] have further advanced multi-frame detection and tracking. Recently, attention-guided multi-task networks and end-to-end streak-like target detectors [19], [20] were introduced. However, most methods depend on complex models, resulting in a challenge for single-frame detection under low signal-to-noise ratio.

Our motivation is to leverage temporal consistency priors of targets to detect space objects. It is implemented by two stages, single-frame detection and cross-frame trajectory completion. The contributions of this paper are summarized as follows:

- We propose a matching-centric sequential post-processing framework. The Hungarian algorithm stabilizes cross-frame association is combined with statistical gating, neighborhood support filtering, and hierarchical completion to balance precision and recall in GEO scenarios.
- We present an adaptive threshold estimation and gating mechanism, which integrates prior knowledge and online statistics. It enhances the method's robustness against distribution changes and device noise.
- Experiments on the SpotGEO dataset demonstrate that our method achieves an  $F_1$  score of 90.14%, outperforming the baseline approaches. Ablation experiments validate the fundamental role of Hungarian matching in the entire pipeline.

## II. METHODOLOGY

The overall framework of our method is illustrated in Fig. 1. It first performs label transformation on the dataset, then en-

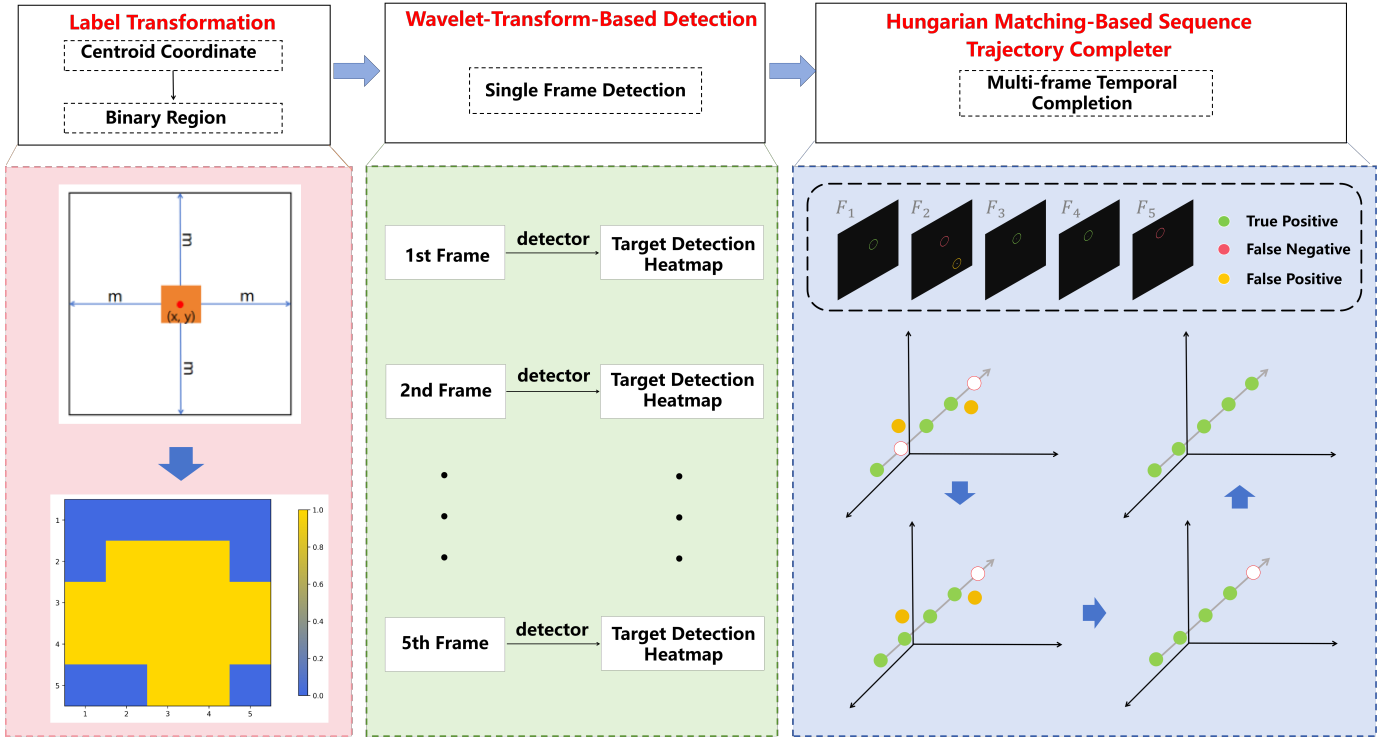


Fig. 1. The framework of the proposed method. Stage 1 generates adaptive binary maps through dataset label transformation; Stage 2 is single-frame detection via wavelet-transform-based feature enhancement; Stage 3 is multi-frame temporal completion.

hances GEO target features through wavelet transform. Finally, it refines the single-frame detection results using a carefully designed sequential trajectory completer, thereby effectively improving the performance of space object detection.

#### A. Transformation of Dataset Labels

The SpotGEO dataset released by the ESA provides only centroid coordinates of space objects. However, factors such as long exposure and atmospheric refraction cause targets to appear as diffuse regions encompassing both center points and surrounding pixels. By selecting higher-intensity pixels near the center, we can enhance annotation information and further improve detection accuracy. Using fixed-size rectangular sub-images as labels fails to accommodate varying target sizes and introduces erroneous pixel-level annotations, which adversely affects network training. We therefore implemented region-based fine-grained filtering for label transformation, as illustrated in Fig. 2.

For a center point  $(x, y)$ , we first expand  $m$  pixels in all directions to form a square local window with side length of  $2m + 1$ . The grayscale values within this window are then normalized to the range  $[0, 1]$  and binarized using a threshold of 0.5, where pixels exceeding 0.5 are considered as the effective region of objects. Subsequently, we apply mild morphological dilation to the binary mask using a circular structuring element of radius 1 to connect weak streak discontinuities and bridge sparse bright spots. The binary map serves as the shape label. Unlike fixed-size rectangular patches, it

covers the distinguishable brightness region around the center without overextending into the background.

#### B. Single Frame Detection Based on Wavelet-Transform Algorithm

This paper proposes a Wavelet Transform-based network for space object detection (WTNet) that incorporates wavelet feature enhancement during the single-frame detection stage [21], [22]. The core implementation of the network relies on the multi-scale feature processing mechanism of the wavelet feature enhancement module. First, the input features are decomposed via wavelet transform into low-frequency (LL) and high-frequency (LH, HL, HH) components. The high-frequency components undergo convolutional enhancement and scale adjustment to accentuate target edge information, while the low-frequency components preserve object contours. Subsequently, the enhanced features are reconstructed through inverse wavelet transform and fused with base convolutional features via residual connections. Finally, the CBAM attention mechanism is introduced to recalibrate the fused features along channel and spatial dimensions. The network adopts an encoder-decoder architecture overall, achieving mapping from raw images to target detection heatmaps through multi-scale feature fusion and skip connections, thereby providing more robust feature representation for space objects.

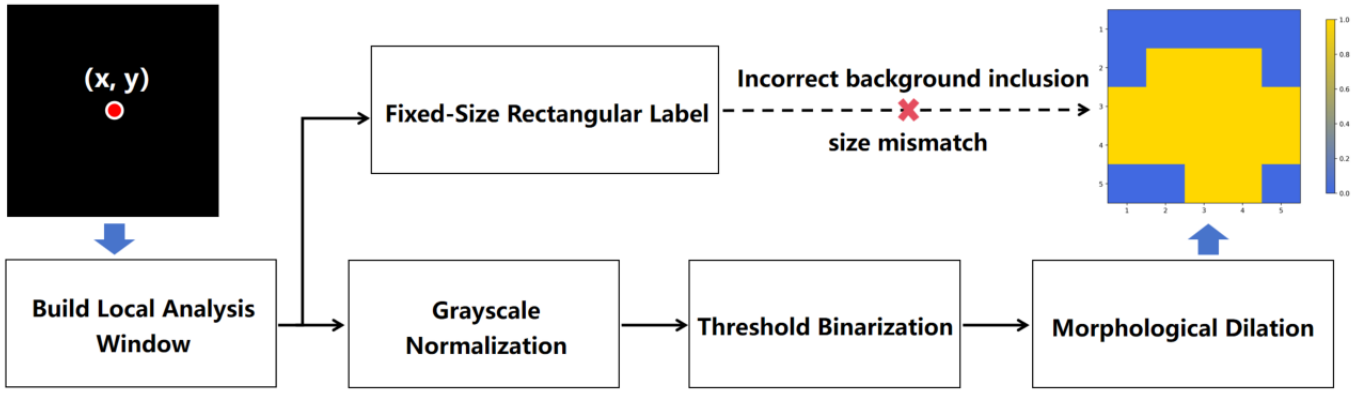


Fig. 2. Flowchart of dataset label transformation.

### C. Trajectory Processing Based on Multi-frame Temporal Completion Algorithm

For detection task characterized by faint features and complex backgrounds, single-model approaches often struggle to achieve a satisfactory balance between recall and precision. Consequently, leveraging multi-frame temporal priors of space objects, we design a sequential trajectory completer centered on the Hungarian matching algorithm. As shown in Fig. 1, this completer effectively restores trajectory continuity and enhances robustness through a three-step pipeline comprising temporal matching and interpolation completion, temporal-consistency-based noise filtering, progressive trajectory refinement.

First, interpolation-based completion is performed using temporal matching. For every pair of consecutive frames with detections ( $f_1, f_2$ ) in the sequence, the interpolation process is triggered only when their frame gap is less than 3. Given the sets of detection points  $D_{f_1} = \{p_i = (x_i, y_i)\}$  and  $D_{f_2} = \{q_j = (x_j, y_j)\}$  in frames  $f_1$  and  $f_2$ , a cost matrix  $\mathbf{C} \in \mathbb{R}^{m \times n}$  is constructed (where  $m$  and  $n$  denote the numbers of detection points in the two frames, respectively), with each element  $C_{ij} = \|q_j - p_i\|_2$ . The Hungarian algorithm is employed to obtain an optimal set of matched pairs  $\{(p_i, q_j)\}$  that minimizes the total cost. Linear interpolation is then applied to these pairs to estimate positions in the missing intermediate frames. Defining the interpolation coefficient as  $\alpha = \frac{f-f_1}{f_2-f_1}$  (where  $\alpha \in (0, 1)$ ), the interpolated position in the missing frame  $f$  is given by:

$$\hat{p}_f = p_i + \alpha \cdot (q_j - p_i) \quad (1)$$

To remove residual noise from the sequences, we employ a temporal support degree principle. For each detection point  $p_f$  in frame  $f$  of the sequence, a temporal window  $W = [f - w, f + w]$  (where  $w$  is the window radius) is defined to constrain the temporal scope for support evaluation. The valid frames within the window are  $f' \in W \setminus \{f\}$ . For each valid frame  $f'$  in the window, the distances  $d$  between  $p_f$  and all detection points in frame  $f'$  are computed. If there exists a detection point satisfying  $d \leq \tau$  (where  $\tau$  is the spatial distance

threshold), frame  $f'$  is considered to provide valid support for  $p_f$ . The number of valid supporting frames  $S$  within the window is counted, and the support ratio is calculated as:

$$r = \frac{S}{N} \quad (2)$$

For each point, if its support ratio is below a threshold and the sequence length exceeds 3, it is identified as an isolated noise point and removed from the sequence. Otherwise, it is retained as a genuine target point with reliable temporal support. Additionally, all detection points are preserved when the sequence length is less than or equal to 3 to avoid excessive filtering.

Since prolonged target occlusion and sudden drops in signal-to-noise ratio still cause missed detections in the sequence, we adopt a progressive trajectory completion approach that incrementally completes missing points from conservative to aggressive strategies. Based on the statistical characteristics of inter-frame distances and the maximum trajectory distance, an adaptive threshold  $T_{\text{stat}}$  is constructed and further extended to define the regular completion threshold  $T_{\text{comp}}$  and the aggressive completion threshold  $T_{\text{agg}}$ . Using the target frame as a reference, the preceding three frames are selected as reference frames. Valid matching pairs are then filtered based on Euclidean distance, followed by the computation and normalization of displacement vectors for each frame. Here,  $i$  denotes the frame interval between the reference frame and the target frame, while  $(x_{\text{ref}}, y_{\text{ref}})$  and  $(x_{\text{check}}, y_{\text{check}})$  represent the coordinates of the target frame and reference frame, respectively.

$$\vec{v} = \left( \frac{x_{\text{ref}} - x_{\text{check}}}{i}, \frac{y_{\text{ref}} - y_{\text{check}}}{i} \right) \quad (3)$$

For scenarios with dual-end constraints, interpolation completion is employed. The Hungarian algorithm is used to match the preceding ( $f_{\text{prev}}$ ) and succeeding ( $f_{\text{next}}$ ) frames, retaining pairs with a distance less than  $T_{\text{comp}}$ . The interpolation coordinates are then calculated based on the temporal proportion:

$$\begin{aligned} (x_{\text{interp}}, y_{\text{interp}}) &= (x_{\text{prev}} + \alpha(x_{\text{next}} - x_{\text{prev}}), \\ &\quad y_{\text{prev}} + \alpha(y_{\text{next}} - y_{\text{prev}})) \end{aligned} \quad (4)$$

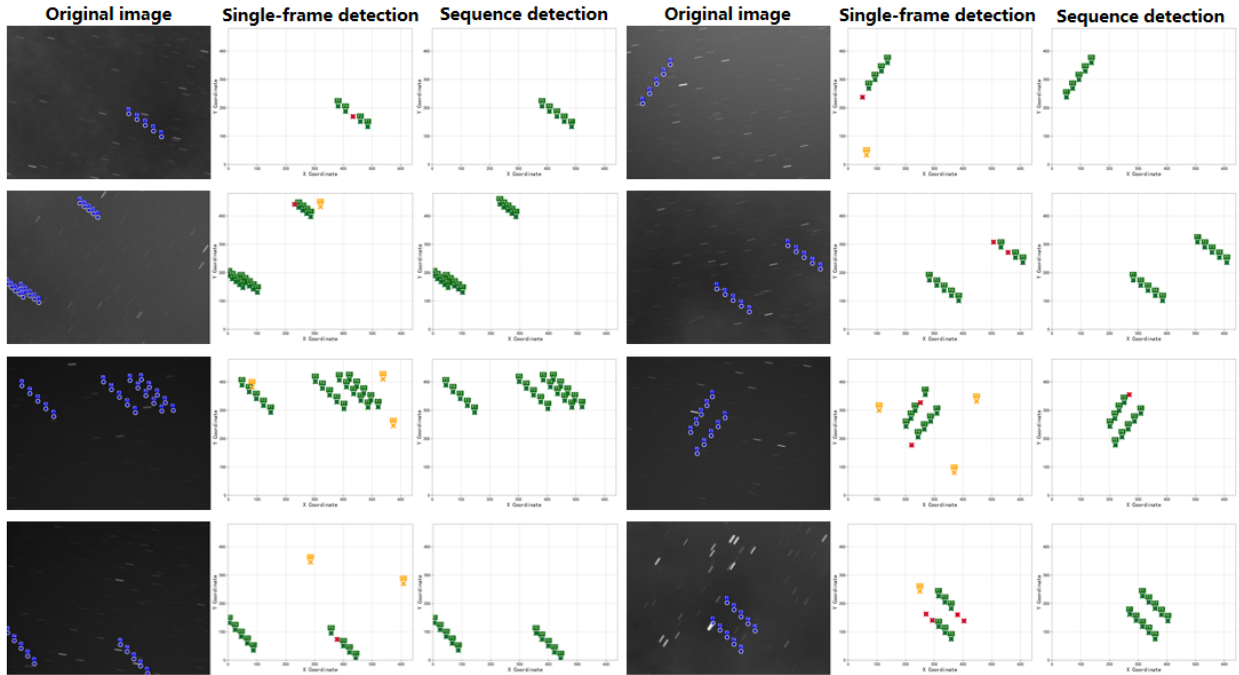


Fig. 3. Visual results of sequential detection. The left column are original observation frames; the middle column are single-frame detection results; the right column are the final detection results after multi-frame temporal trajectory completion. The blue dots denote ground truth, the green dots represent true positives, the yellow dots indicate false positives, and red dots correspond to false negatives.

For single-end constraint scenarios, motion vector-based extrapolation is applied, where  $\Delta f$  denotes the number of intervening frames, and  $\vec{v}_x$ ,  $\vec{v}_y$  represent the components of the motion vector:

$$(x_{\text{extrap}}, y_{\text{extrap}}) = (x_{\text{ref}} + \vec{v}_x \cdot \Delta f, y_{\text{ref}} + \vec{v}_y \cdot \Delta f) \quad (5)$$

In cases of weak constraints (significant missing data), an aggressive completion strategy is adopted, which utilizes linear regression to model the temporal-spatial correlation of available detections.

### III. EXPERIMENTS

#### A. Experimental Setup

Experiments were conducted on the public SpotGEO dataset. Evaluation metrics included the  $F_1$  score and Mean Square Error (MSE). We implemented our model using a U-net architecture [23] within the PyTorch framework. The model was trained for 400 epochs using the AdamW optimizer, with the learning rate dynamically adjusted by a cosine annealing strategy and initialized at 0.0015. All experiments were performed on an NVIDIA GeForce RTX 3090 GPU.

#### B. Quantitative Analysis

We conducted a systematic assessment on the SpotGEO dataset and compared it with several single-frame detection algorithms. Table I presents the comparative results of different object detectors. It indicates that the proposed WTNet achieves an  $F_1$  score of 88.07% and outperforms other methods.

To validate the effectiveness of the sequential trajectory completion module, we test different post-processing strategies. Experimental results indicate that combining single-frame detection with spatial point clustering alleviated false alarms to some extent, achieving an  $F_1$  of 88.56%. However, due to the lack of a trajectory-level constraint mechanism, inter-frame mismatch remained noticeable. To address this, Hungarian matching-based trajectory completion strategy establishes one-to-one correspondences between consecutive frames and performs completion for missing trajectories. This strategy ultimately makes our method achieve the  $F_1$  to 90.14% while reducing the MSE to 61958.1973.

TABLE I  
PERFORMANCE COMPARISON OF 2D SINGLE-FRAME OBJECT DETECTORS.

Methods	F1(%)	MSE
Resnet18	75.43	259633.7200
Faster R-CNN	80.19	162168.6600
Cascade R-CNN	82.54	177082.0900
YOLOv3	81.89	141504.5600
PP-YOLO	82.21	181461.1300
PP-YOLOv2	84.08	160997.9800
PP-YOLO-SOD	83.97	140923.2000
WTNet(ours)	88.07	213183.4354

#### C. Visual Results

Fig. 3 presents the sequential detection results of our method on the SpotGEO dataset. The selected eight sequences include both single-target and multi-target detection scenarios. Close

observation reveals that during the single-frame detection stage, the wavelet transform module effectively enhances the high-frequency features of space objects, maintaining distinct separability against strong stellar backgrounds and high-noise interference, while achieving precise candidate point localization. After incorporating Hungarian matching for multi-frame trajectory fitting and completion, the system successfully restores trajectory continuity and integrity even in challenging conditions including dense star fields, low signal-to-noise ratios, and partial occlusion, significantly reducing the probabilities of missing detections.

#### IV. CONCLUSION

In this paper, we propose a framework based on single-frame detection and multi-frame temporal trajectory completion strategy. The proposed WNet achieves an  $F_1$  of 88.07%, outperforming the typical single-frame detection approaches. Visual results demonstrate the effectiveness of the multi-frame temporal trajectory completion strategy, which can predict missed objects accurately and reduce false detections. This combination of single-frame detection and temporal completion strategy is promising to improve space object detection. In future, this can be invested to improve the model's robustness across diverse observational scenarios and complex space environments.

#### REFERENCES

- [1] C. Toth and G. Józskó, "Remote sensing platforms and sensors: a survey," *ISPRS Journal of Photogrammetry and Remote Sensing*, vol. 115, pp. 22–36, 2016.
- [2] T. S. Abdu, S. Kisseleff, E. Lagunas, and S. Chatzinotas, "Flexible resource optimization for geo multibeam satellite communication system," *IEEE Transactions on Wireless Communications*, vol. 20, no. 12, pp. 7888–7902, 2021.
- [3] J. Li *et al.*, "A review of recent development of geosynchronous synthetic aperture radar technique," *Remote Sensing*, vol. 17, no. 20, p. 3405, 2025.
- [4] D. Li, S. Wu, Y. Wang, W. Wu, and Q. Zhang, "Intelligent task scheduling in hybrid geo-leo satellite-assisted marine iot network," *IEEE Internet of Things Journal*, vol. 12, no. 7, pp. 8353–8367, 2025.
- [5] J. Fitzmaurice, D. Bédard, C. H. Lee, and P. Seitzer, "Detection and correlation of geosynchronous objects in nasa's wide-field infrared survey explorer images," *Acta Astronautica*, vol. 183, pp. 176–198, 2021.
- [6] J. Xue, Y. Zhang, X. Tao, and S. Zhao, "Research on space object origin tracing approach using density peak clustering and distance feature optimization," *Applied Sciences*, vol. 15, no. 20, p. 10943, 2025.
- [7] D. Liu, B. Chen, T.-J. Chin, and M. G. Rutten, "Topological sweep for multi-target detection of geostationary space objects," *IEEE Transactions on Signal Processing*, vol. 68, pp. 5166–5177, 2020.
- [8] B. Chen *et al.*, "Spot the geo satellites: from dataset to kelvins spotgeo challenge," in *Proceedings of the 2021 IEEE/CVF Conference on Computer Vision and Pattern Recognition Workshops (CVPRW)*. Nashville, TN, USA: IEEE, 2021, pp. 2086–2094.
- [9] X. Wang *et al.*, "Star suppression based on structure of star groups for geosynchronous object detection using wide-field telescopes," *IEEE Transactions on Aerospace and Electronic Systems*, vol. 60, no. 3, pp. 3160–3176, 2024.
- [10] L. Guo, W. Zhang, Z. Wang, X. Sun, and Y. Shang, "Weak geo satellite target detection based on image transformation and energy accumulation," in *Proceedings of the 4th International Conference on Image and Graphics Processing*. New York: ACM, 2021, pp. 52–58.
- [11] F. Wu *et al.*, "Attention-guided multi-task network for streak-like dim and small space target detection in single optical images," *Advances in Space Research*, 2025.
- [12] B. Wang, Y. Zhao, and C. L. P. Chen, "Hybrid transfer learning and broad learning system for wearing mask detection in the covid-19 era," *IEEE Transactions on Instrumentation and Measurement*, vol. 70, pp. 1–12, 2021.
- [13] Q. Mao *et al.*, "Spirdet: toward efficient, accurate, and lightweight infrared small-target detector," *IEEE Transactions on Geoscience and Remote Sensing*, vol. 62, pp. 1–12, 2024.
- [14] R. Abay and K. Gupta, "Geo-fpn: a convolutional neural network for detecting geo and near-geo space objects from optical images," in *Proceedings of the 8th European Conference on Space Debris*. Darmstadt, Germany: ESA Space Debris Office, 2021, pp. 123–129.
- [15] Y. Jiang, Y. Tang, and C. Ying, "Finding a needle in a haystack: faint and small space object detection in 16-bit astronomical images using a deep learning-based approach," *Electronics*, vol. 12, no. 23, p. 4820, 2023.
- [16] Y. Dai, T. Zheng, C. Xue, and L. Zhou, "Effective multi-frame optical detection algorithm for geo space objects," *Applied Sciences*, vol. 12, no. 9, pp. 4610–4626, 2022.
- [17] J. Liu, F. Yu, Y. Yuan, and Y. Yang, "Multi-frame temporal dense nested attention method for detecting geo objects," *Advances in Space Research*, vol. 75, no. 9, pp. 6911–6923, 2025.
- [18] S. Chen, H. Wang, Z. Shen, K. Wang, and X. Zhang, "Convolutional long-short term memory network for space debris detection and tracking," *Knowledge-Based Systems*, vol. 304, p. 112535, 2024.
- [19] Y. Han, D. Wen, J. Li, and Z. Qiao, "Improved detection of multiple faint streak-like space targets in a single star image," *Remote Sensing*, vol. 17, no. 4, p. 631, 2025.
- [20] G. Zhuang *et al.*, "High performance space debris tracking in complex skylight backgrounds with a large-scale dataset," *arXiv preprint*, 2025.
- [21] B. Xin, Q. Li, Q. Mao, J. Wang, and B. Wang, "Fbi-net: frequency band integration network for infrared small target segmentation," in *ICASSP 2025 - 2025 IEEE International Conference on Acoustics, Speech and Signal Processing (ICASSP)*. Hyderabad, India: IEEE, 2025, pp. 1–5.
- [22] B. Wang, C. Li, W. Zou, and Q. Zheng, "Foreign object detection network for transmission lines from unmanned aerial vehicle images," *Drones*, vol. 8, no. 8, p. 361, 2024.
- [23] O. Ronneberger, P. Fischer, and T. Brox, "U-net: convolutional networks for biomedical image segmentation," in *Medical Image Computing and Computer-Assisted Intervention – MICCAI 2015*. Cham: Springer International Publishing, 2015, pp. 234–241.